analytical chemistry

pubs.acs.org/ac

Letter

A Novel ECL Sensing System for Ultrahigh Sensitivity miRNA-21 Detection Based on Catalytic Hairpin Assembly Cascade Nonmetallic SPR Effect

Jingxian Li, Ren Cai,* and Weihong Tan

Cite This: *Anal. Chem.* 2022, 94, 12280−12285

Read Online

ACCESS | Metrics & More | Article Recommendations | Supporting Information

ABSTRACT: A novel electrochemical luminescence (ECL) sensing system is designed based on the catalytic hairpin assembly (CHA) cascade nonmetallic surface plasmon resonance (SPR) effect for ultrasensitive and selective miRNA-21 detection. In the CHA cycles, much more target miRNA-21 is captured to amplify the detection signal and enhance sensitivity. Meanwhile, the specific recognition between streptavidin (SA) and biotin, together with the SPR effect of SnS_2 nanoplates on perylene tetracarboxylic acid, further amplifies the ECL signal. Together, miRNA-21 can be quantified with a limit of detection of 0.6 aM in the novel ECL system with ultrahigh sensitivity and selectivity. The ECL biosensor exhibits excellent stability and reproducibility as well as good practicality for miRNA-21 detection in real human serum.

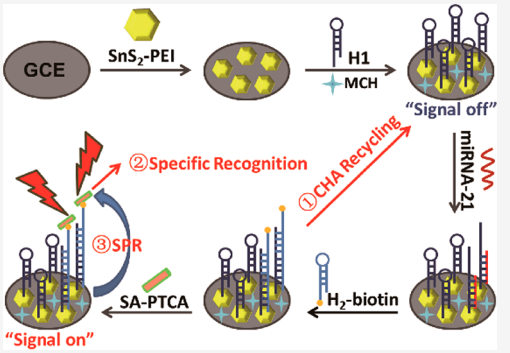

INTRODUCTION

MicroRNAs (miRNAs), a class of small and nonprotein-coding RNA molecules containing about 19−24 nucleotides, play an extremely important role in the regulation of various biological processes and gene expression.[1−4] miRNA-21 is widely presented in lung cancer, breast cancer, cervical cancer, colorectal cancer, prostate cancer, and other tumor cells, and it shows high concentrations in these cells.[5,6] Therefore, accurate and sensitive detection of miRNA-21 is of great value for the early diagnosis and treatment of tumors. Up to now, numerous analytical methods have been developed to monitor miRNA-21, such as Northern blotting,[7] quantitative reverse transcription-polymerase chain reaction (qRT-PCR),[8] colorimetrics,[9,10] surface-enhanced Raman,[11,12] and electrochemical methods.[13,14] For example, a microfluidic surface-enhanced Raman scattering (SERS) sensor was designed for microRNA detection by a nucleic acid-tyramine cascade amplification.[15] A photoelectrochemical biosensor was proposed for miRNA-21 based on a b-TiO_2/CdS:Eu/Ti_3C_2 heterojunction.[16] In addition, sensitive electrochemiluminescence analysis of miRNA-21 was achieved by a reversible addition-fragmentation chain transfer (RAFT) signal amplification.[17]

Electrochemical luminescence (ECL), as an effective analytical method, integrates the merits of both electrochemistry and chemiluminescence and has aroused attention in early disease diagnosis and detection of hazardous substances due to its low signal background, high sensitivity, and simple operation.[18−20] Meanwhile, catalytic hairpin assembly (CHA) technology, an enzyme-free and constant temperature nucleic acid signal amplification technology,[21] is often combined with the ECL method to achieve ultrahighly sensitive and selective detection of biomolecules. For example, an ultrasensitive biosensor was designed to detect miRNA-21 by the combination of CHA and the surface plasmon-enhanced ECL (SPEECL) of silver nanoclusters.[22] A biosensor was exploited by combining CHA amplification strategy with CRISPR-Cas12a side-cutting feature to achieve sensitive amplification assay of Siglec-5 with LOD of 29.36 fM.[23]

In order to further improve the sensitivity of the ECL biosensor and avoid false positive results, as a potential approach, surface plasmon resonance (SPR) technology was introduced into the ECL-CHA system. Based on its merits of excellent sensitivity and simplicity,[24,25] SPR technology has been broadly utilized in many sensing applications, such as pH sensors,[26] fluorescence sensors,[27] organic vapor sensors,[28] and electrochemical sensors.[29] To our knowledge, nonmetallic materials are rarely reported as the plasma source to facilitate the ECL performance because of their relatively poor electrical conductivity.[30,31] However, the nonmetallic sulfides, e.g., MoS_2 and Cu_2S, have surface plasmon effects in the visible and near-infrared regions, with the advantages of easy preparation, low toxicity, and good biocompatibility.[32] Thus, SnS_2 nanoplates would be good potential plasma sources to enhance the ECL

Received: July 25, 2022
Accepted: August 30, 2022
Published: August 31, 2022

https://doi.org/10.1021/acs.analchem.2c03238
Anal. Chem. 2022, 94, 12280−12285

signal of the luminophore. On the other hand, perylene tetracarboxylic acid (PTCA), a five-ring polycyclic aromatic hydrocarbon rich in carboxyl groups, is always considered to be a promising ECL luminophore with its large π-conjugated system, broad absorption wavelength range, and good film-forming properties,[33,34] all of which make PTCA an appropriate luminophore candidate.

Herein, a novel ECL platform for miRNA-21 assay is proposed using CHA and SPR technology based on the SnS_2 nanoplates as a plasma source and PTCA as a luminophore (Scheme 1). Here, CHA cycles amplify the detection signal to

Scheme 1. (a) Preparation of SnS_2-PEI and (b) Design of ECL Biosensor for miRNA-21 Assay

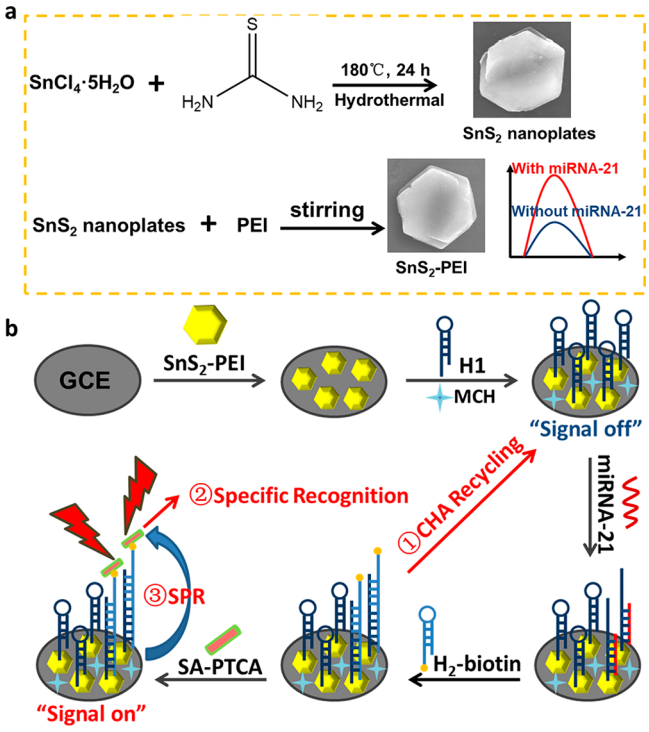

enhance sensitivity by capturing much more target miRNA-21. Meanwhile, the specific recognition between streptavidin (SA) and biotin, and the SPR effect of SnS_2 nanoplates on PTCA further amplify the ECL signal. As a result, miRNA-21 can be quantified with ultrahigh sensitivity and selectivity in the novel ECL system based on the CHA cycles cascade SPR effect. In addition, this ECL biosensor shows great practical potential in real sample analysis.

RESULTS AND DISCUSSION

In Figure 1a,b, the scanning electron microscopy (SEM) images of PTCA exhibit nanorod-like structures with widths of 40 nm and lengths of 200 nm. The SEM image of SA-PTCA is shown in Figure S1a; the surface of SA-PTCA is covered with streptavidin. In Figure S1b, the ζ-potentials of PTCA, SA, and SA-PTCA are −0.481, +9.67, and +0.367 mV, respectively, which further confirm the successful preparation of SA-PTCA. Hexagonal nanoplate SnS_2-PEI with diameters of 600 nm consistent with the morphology of SnS_2 are shown in Figure 1d,e.[35] In addition, X-ray photoelectron spectroscopy (XPS) was performed to confirm the successful preparation of PTCA and SnS_2-PEI. The XPS spectrum shows that PTCA contains the elements C and O in Figure 1c and Figure S2. The XPS spectra of SnS_2-PEI in Figure 1f and Figure S3 confirm the existence of Sn, S, C, N, and O elements. Moreover, X-ray diffraction (XRD) and Fourier transform infrared spectroscopy (FT-IR) of PTCA and SnS_2-PEI further prove the successful preparation of PTCA and SnS_2-PEI (Figure S4).

Cyclic voltammetry (CV) and electrochemical impedance spectroscopy (EIS) tests were carried out in 5.0 mM $[Fe(CN)_6]^{3-/4-}$ solution (0.1 M KCl). Figure 2a shows that the maximum peak current of the SnS_2-PEI obviously decreases after successive decoration of hairpin DNA1 (H1), miRNA-21, and hairpin DNA2-biotin (H2-biotin) on the electrode surface. This indicates that the H1 structure was opened and triggered the steric hindrance effect.[36] Moreover, the peak current continuously decreased with the addition of streptavidin-decorated PTCA (SA-PTCA), which can be ascribed to the specific recognition of SA and biotin. The EIS spectrum shows that the resistance value (Ret) increased after the modification of H1, miRNA-21, H2-biotin, and SA-PTCA step-by-step (Figure 2b). This can be attributed to the biomacromolecules (i.e., H1, miRNA-21, H2, and SA) which would impede electron and proton transport on the electrode surface.[37] These results provide strong evidence that the ECL biosensor was successfully fabricated.

The signal amplification strategy of the ECL biosensor is demonstrated in Figure 3 and Figures S5 and S6. There is significant spectral overlap between the ECL emission spectrum of PTCA and the UV−vis absorption spectrum of SnS_2-PEI, thus indicating the existence of a resonance energy transfer (RET) system between PTCA and SnS_2-PEI (Figure 3a).[38] Next, the ECL performance was investigated. As shown in Figure 3b, the ECL intensity increases by 3.64 times in the presence of SnS_2-PEI compared to the case with no SnS_2-PEI. Since the distance between the PTCA and SnS_2-PEI is larger than 20 nm,[22] the SPR effect of SnS_2-PEI must have been activated to amplify the ECL signal for the biosensor.

The signal amplification process can be depicted as follows. First, the $S_2O_8^{2-}$ and PTCA react to generate $SO_4^{\bullet-}$ and $PTCA^{\bullet-}$ (eq 1 and eq 2). Next, $SO_4^{\bullet-}$ and $PTCA^{\bullet-}$ further react to produce PTCA* (eq 3). When PTCA* returns to the ground state, an ECL signal is observed at the cathode (eq 4). After the modification of SA-PTCA, a highly strong ECL signal can be observed owing to the specific recognition of SA and biotin to induce the SPR effect of SnS_2-PEI on the PTCA.

$$S_2O_8^{2-} + e^- \rightarrow SO_4^{\bullet-} + SO_4^{2-} \quad (1)$$

$$PTCA + e^- \rightarrow PTCA^{\bullet-} \quad (2)$$

$$SO_4^{\bullet-} + PTCA^{\bullet-} \rightarrow PTCA^* + SO_4^{2-} \quad (3)$$

$$PTCA^* \rightarrow PTCA + h\nu \quad (4)$$

The effects on ECL performance of the pH value of PBS, incubation temperature, the concentration variation of SnS_2-PEI, and the incubation time of the hairpin DNA were investigated, as shown in Figure 4a−d, respectively. The results show that pH 7.5 of PBS, 37 °C incubation temperature, 2 mg·mL^{-1} of SnS_2-PEI, and a 2 h incubation time provide the optimal experimental conditions. The ECL signal is continuously amplified with the increment of the miRNA-21 concentration (Figure 5a), and there is a good linear relationship between the ECL signal and the logarithm of the miRNA-21 concentration (lg $c_{miRNA-21}$, fM) (Figure 5b).

https://doi.org/10.1021/acs.analchem.2c03238
Anal. Chem. 2022, 94, 12280−12285

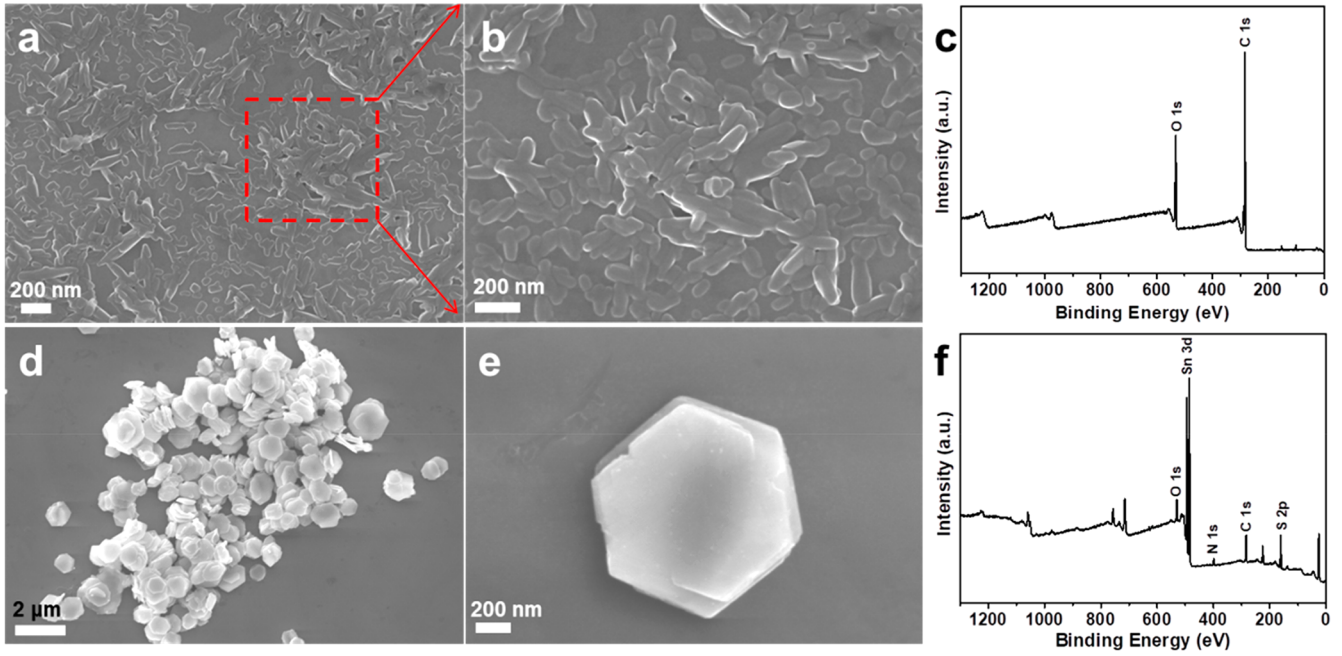

Figure 1. SEM images (a, b, d, e) and XPS patterns (c, f) of PTCA and SnS_2-PEI.

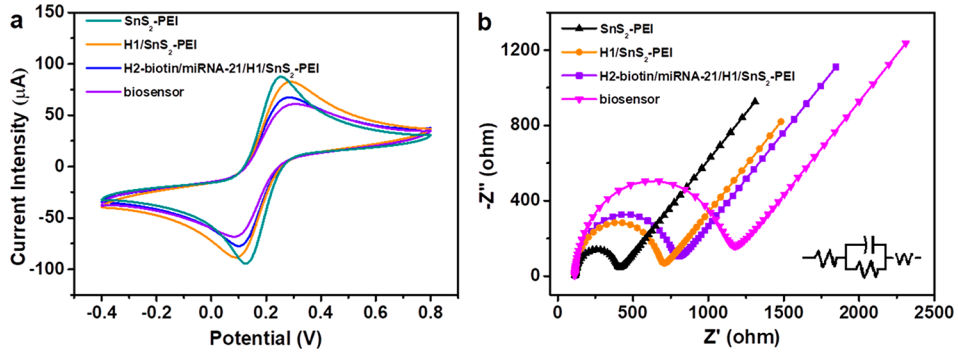

Figure 2. (a) CV and (b) EIS profiles of SnS_2-PEI/GCE, H1/SnS_2-PEI, H2-biotin/miRNA-21/H1/SnS_2-PEI/GCE, SA-PTCA/H2-biotin/miRNA-21/H1/SnS_2-PEI/GCE.

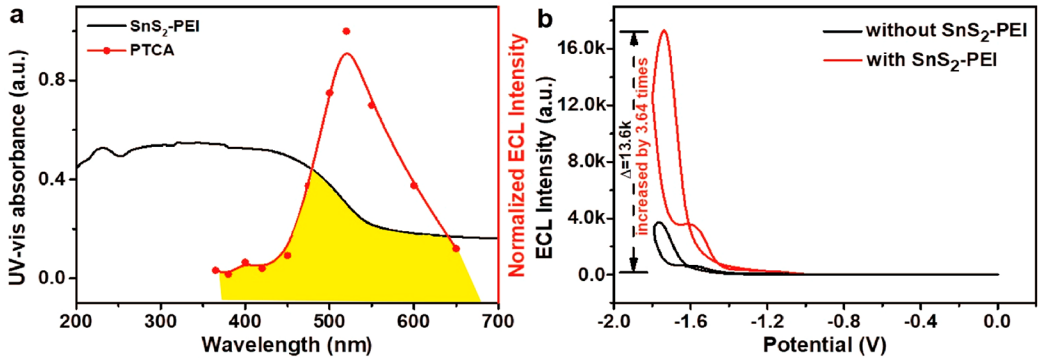

Figure 3. UV−vis absorption and ECL emission spectra of (a) SnS_2-PEI and PTCA; (b) ECL profiles of the biosensor without and with SnS_2-PEI.

The linear equation is fitted as $I = 1481.73 \lg c + 10\,322$ with a correlation coefficient 0.9934, and the limit of detection (LOD) is calculated as 0.6 aM (S/N = 3).[39] In Figure 5c, the ECL intensities with 10 nM concentrations of possible interferences (miRNA-141, miRNA-182, miRNA-126) are almost the same as the blank, while the ECL intensity is greatly enhanced in the presence of target miRNA-21 (1 nM), indicating the good specificity of the ECL biosensor. In Figure 5d, the ECL intensity shows no variation when the biosensor was tested in 20 consecutive CV scans in the presence of target miRNA-21 (1 aM, 100 fM, and 1 nM), thus demonstrating the excellent stability for the ECL biosensor. In addition, the good reproducibility and long-time stability of the ECL biosensor are confirmed in Figure S7.

https://doi.org/10.1021/acs.analchem.2c03238
Anal. Chem. 2022, 94, 12280−12285

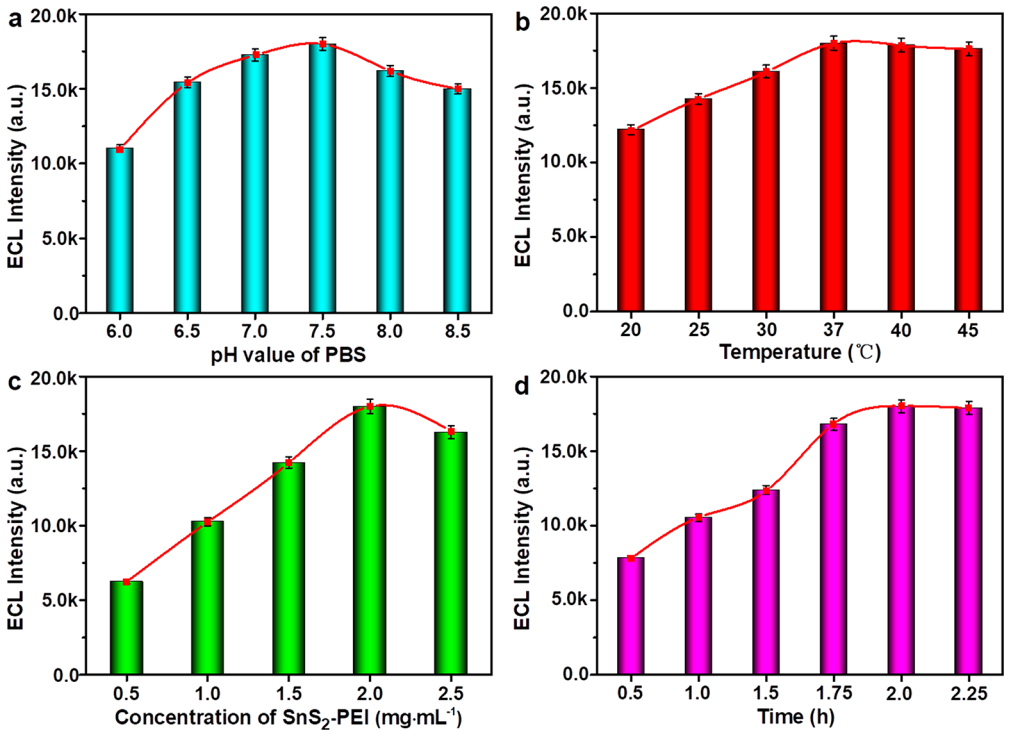

Figure 4. Effects of (a) pH value of PBS, (b) incubation temperature, (c) SnS_2-PEI concentration, and (d) incubation time of hairpin DNA on the performance of the ECL biosensor.

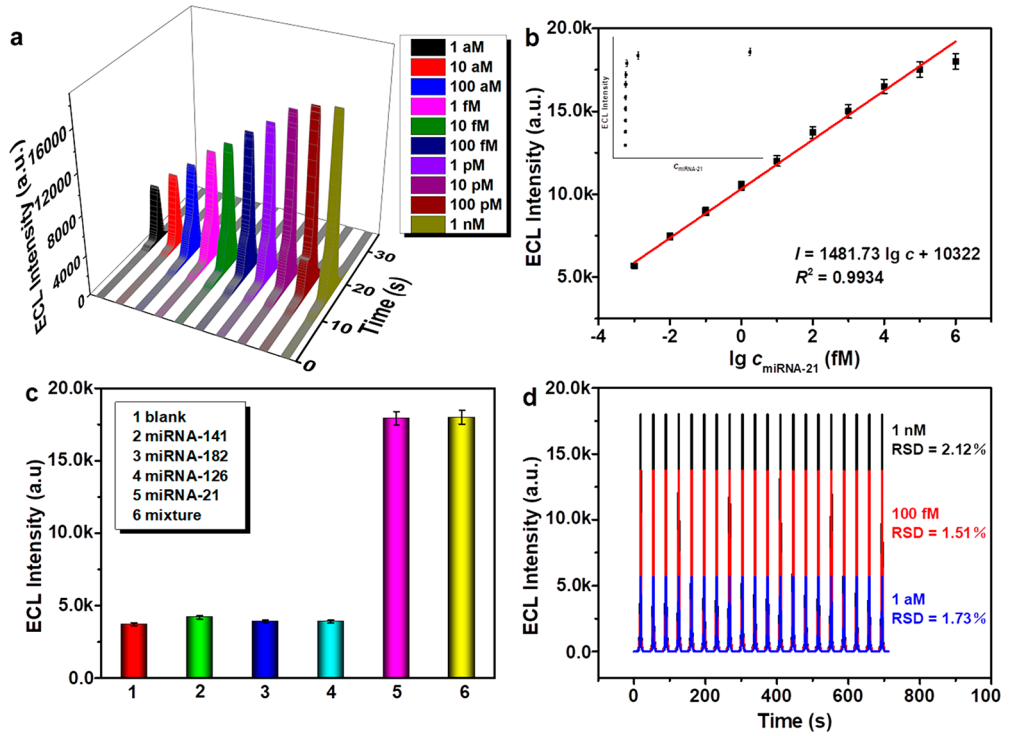

Figure 5. (a) ECL response toward different concentrations of miRNA-21. (b) Calibration curve for quantification of miRNA-21 from 1 aM to 1 nM. (c) Selectivity and (d) stability of the ECL biosensor with 1 aM, 100 fM, and 1 nM miRNA-21.

To validate the practicability of the ECL biosensor, a standard addition method was applied to detect miRNA-21 with different concentrations: 10 aM, 100 aM, and 1 fM in 1000-fold diluted human serum samples. In Table S1, the recovery rates are calculated to be 95.00% ~ 102.4%, while the relative standard deviation are 1.99−3.24%. Thus, this ECL biosensor exhibits very good applicability for the miRNA-21 detection in real human serum samples. Compared with the previous analytical methods for miRNA-21 assay, this work displays a wider detection range with superior sensitivity (Table S2).

https://doi.org/10.1021/acs.analchem.2c03238
Anal. Chem. 2022, 94, 12280−12285

CONCLUSIONS

In summary, a novel ECL sensing platform is successfully designed with the CHA cycles cascade SPR effect for superior sensitivity and selective detection of miRNA-21 with a LOD of 0.06 aM. The SnS_2-PEI exerts a strong SPR effect on the luminophore PTCA, and the CHA cycles capture much more target miRNA-21 to amplify the detection signal and enhance sensitivity. Together, the strong SPR effect and CHA cycles lead to ultrasensitive quantification of miRNA-21. Furthermore, the ECL biosensor exhibits excellent analytical performance in view of selectivity, stability, reproducibility, and practicability in real samples. This work serves as a model for the application of CHA cycles cascade SPR technology to design ultrahighly sensitive ECL platforms for disease diagnosis.

ASSOCIATED CONTENT

Supporting Information

The Supporting Information is available free of charge at https://pubs.acs.org/doi/10.1021/acs.analchem.2c03238.

Experimental details, materials, preparation of PTCA and SA-PTCA, preparation of SnS_2-PEI, fabrication of the ECL biosensor, LOD calculation, XPS spectrum, XRD and FT-IR spectrum, UV−vis absorption spectra, determination of miRNA-21 in human serum samples, comparison of different analytical methods (PDF)

AUTHOR INFORMATION

Corresponding Author

Ren Cai − *Molecular Science and Biomedicine Laboratory, State Key Laboratory for Chemo/Bio-Sensing and Chemometrics, College of Material Science and Engineering, College of Chemistry and Chemical Engineering, College of Biology, Hunan University, Changsha 410082, China;* orcid.org/0000-0003-2583-7133; Email: cairen@hnu.edu.cn

Authors

Jingxian Li − *Molecular Science and Biomedicine Laboratory, State Key Laboratory for Chemo/Bio-Sensing and Chemometrics, College of Material Science and Engineering, College of Chemistry and Chemical Engineering, College of Biology, Hunan University, Changsha 410082, China*

Weihong Tan − *Molecular Science and Biomedicine Laboratory, State Key Laboratory for Chemo/Bio-Sensing and Chemometrics, College of Material Science and Engineering, College of Chemistry and Chemical Engineering, College of Biology, Hunan University, Changsha 410082, China; The Cancer Hospital of the University of Chinese Academy of Sciences (Zhejiang Cancer Hospital), Institute of Basic Medicine and Cancer (IBMC), Chinese Academy of Sciences, Hangzhou, Zhejiang 310022, China; Institute of Molecular Medicine, Renji Hospital, Shanghai Jiao Tong University School of Medicine, and College of Chemistry and Chemical Engineering, Shanghai Jiao Tong University, Shanghai 200240, China;* orcid.org/0000-0002-8066-1524

Complete contact information is available at: https://pubs.acs.org/10.1021/acs.analchem.2c03238

Author Contributions

All authors have given approval to the final version of the paper.

Notes

The authors declare no competing financial interest.

ACKNOWLEDGMENTS

This work was supported by the National Natural Science Foundation of China (22004032) and Hunan Provincial Natural Science Foundation of China (2021JJ20020).

REFERENCES

(1) Zhong, M.; Chen, K.; Sun, W.; Li, X.; Huang, S.; Meng, Q.; Sun, B.; Huang, X.; Wang, X.; Ma, X.; Ma, P. *Biosens. Bioelectron.* **2022**, *214*, 114497.

(2) Khashayar, P.; Al-Madhagi, S.; Azimzadeh, M.; Scognamiglio, V.; Arduini, F. *TrAC, Trends Anal. Chem.* **2022**, *156*, 116706.

(3) Liu, C.; An, Y.; Zhang, Y.; Li, X.; Xue, Q.; Wang, H. *Chem. Commun.* **2019**, *55* (91), 13733−13736.

(4) Zhang, G.; Han, Q.; Song, L.; Liu, P.; Kuang, G.; Fu, Y. *Sens. Actuators, B* **2021**, *346*, 130529.

(5) Shin, S.; Jung, Y.; Uhm, H.; Song, M.; Son, S.; Goo, J.; Jeong, C.; Song, J.-J.; Kim, V. N.; Hohng, S. *Nat. Commun.* **2020**, *11* (1), 6033.

(6) Kong, L.; Li, H.; Zhang, X.; Zhuo, Y.; Chai, Y.; Yuan, R. *Anal. Chem.* **2022**, *94* (12), 5167−5172.

(7) Koscianska, E.; Starega-Roslan, J.; Sznajder, L. J.; Olejniczak, M.; Galka-Marciniak, P.; Krzyzosiak, W. J. *BMC Mol. Biol.* **2011**, *12* (1), 14.

(8) Hu, C.; Zhang, L.; Yang, Z.; Song, Z.; Zhang, Q.; He, Y. *Anal. Chim. Acta* **2021**, *1174*, 338715.

(9) Hosseinzadeh, E.; Ravan, H.; Mohammadi, A.; Pourghadamyari, H. *Talanta* **2020**, *216*, 120913.

(10) Wang, L.; Liu, Z.-J.; Cao, H.-X.; Liang, G.-X. *Sens. Actuators, B* **2021**, *337*, 129813.

(11) Kim, W. H.; Lee, J. U.; Jeon, M. J.; Park, K. H.; Sim, S. J. *Biosens. Bioelectron.* **2022**, *205*, 114116.

(12) Han, Y.; Qiang, L.; Gao, Y.; Gao, J.; He, Q.; Liu, H.; Han, L.; Zhang, Y. *Appl. Surf. Sci.* **2021**, *541*, 148456.

(13) Cao, W.; Liu, L.; Yuan, R.; Wang, H. *Biosens. Bioelectron.* **2022**, *214*, 114506.

(14) Hou, Z.; Zheng, J.; Zhang, C.; Li, T.; Chen, D.; Hu, L.; Hu, J.; Xiong, B.; Ye, H.; Jaffrezic-Renault, N.; Guo, Z. *Sens. Actuators, B* **2022**, *367*, 132067.

(15) Zhao, Y.; Fang, X.; Bai, M.; Zhang, J.; Yu, H.; Chen, F.; Zhao, Y. *Chin. Chem. Lett.* **2022**, *33* (4), 2101−2104.

(16) Liu, S.-T.; Chen, J.-S.; Liu, X.-P.; Mao, C.-J.; Jin, B.-K. *Talanta* **2022**, 123601.

(17) Wang, Q.; Yu, S.; Zhang, L.; Wang, L.; Kong, J.; Li, L.; Zhang, X. *Chem. Commun.* **2022**, *58* (11), 1701−1703.

(18) Ma, C.; Cao, Y.; Gou, X.; Zhu, J.-J. *Anal. Chem.* **2020**, *92* (1), 431−454.

(19) Ding, L.; Hong, H.; Xiao, L.; Hu, Q.; Zuo, Y.; Hao, N.; Wei, J.; Wang, K. *Biosens. Bioelectron.* **2021**, *192*, 113492.

(20) Nasrollahpour, H.; Khalilzadeh, B.; Naseri, A.; Sillanpää, M.; Chia, C. H. *Anal. Chem.* **2022**, *94* (1), 349−365.

(21) Liu, Y.; Li, S.; Zhang, L.; Zhao, Q.; Li, N.; Wu, Y. *ACS Omega* **2020**, *5* (20), 11836−11841.

(22) Feng, X.; Han, T.; Xiong, Y.; Wang, S.; Dai, T.; Chen, J.; Zhang, X.; Wang, G. *ACS Sensors* **2019**, *4* (6), 1633−1640.

(23) Zhang, K.; Fan, Z.; Yao, B.; Ding, Y.; Zhao, J.; Xie, M.; Pan, J. *Biosens. Bioelectron.* **2021**, *178*, 113019.

(24) Agrawal, A.; Cho, S. H.; Zandi, O.; Ghosh, S.; Johns, R. W.; Milliron, D. J. *Chem. Rev.* **2018**, *118* (6), 3121−3207.

(25) Mayer, K. M.; Hafner, J. H. *Chem. Rev.* **2011**, *111* (6), 3828−3857.

(26) Li, L.; Zhang, Y. N. *IEEE. T. Instrum. Meas.* **2021**, *70*, 1−9.

(27) Wang, X.; Wang, X.; Liu, Y.; Chu, T.; Li, Y.; Dai, C.; Yang, Y.; Zhang, Y. *Microchem. J.* **2021**, *168*, 106524.
(28) Daly, S. M.; Grassi, M.; Shenoy, D. K.; Ugozzoli, F.; Dalcanale, E. *J. Mater. Chem.* **2007**, *17* (18), 1809−1818.
(29) Li, C.; Han, D.; Liang, Z.; Han, F.; Fu, W.; Wang, W.; Han, D.; Wang, Y.; Niu, L. *Sens. Actuators, B* **2022**, *369*, 132258.
(30) Huo, X.-L.; Zhang, N.; Yang, H.; Xu, J.-J.; Chen, H.-Y. *Anal. Chem.* **2018**, *90* (22), 13723−13728.
(31) Wang, D.; Li, Y.; Lin, Z.; Qiu, B.; Guo, L. *Anal. Chem.* **2015**, *87* (12), 5966−5972.
(32) Liu, Y.; Nie, Y.; Wang, M.; Zhang, Q.; Ma, Q. *Biosens. Bioelectron.* **2020**, *148*, 111823.
(33) Song, X.; Li, X.; Wei, D.; Feng, R.; Yan, T.; Wang, Y.; Ren, X.; Du, B.; Ma, H.; Wei, Q. *Biosens. Bioelectron.* **2019**, *126*, 222−229.
(34) Li, J.; Shan, X.; Jiang, D.; Wang, W.; Xu, F.; Chen, Z. *Microchim. Acta* **2021**, *188* (7), 231.
(35) Zhou, M.; Pu, Y.; Wu, Q.; Wang, P.; Liu, T.; Zhang, M. *Sens. Actuators, B* **2020**, *319*, 319.
(36) Yin, S.; Hossain, M. N.; Li, Y.; Sun, C.; Kraatz, H.-B. *Sens. Actuators, B* **2022**, *354*, 131217.
(37) Han, Q.; Wang, R.; Xing, B.; Zhang, T.; Khan, M. S.; Wu, D.; Wei, Q. *Biosens. Bioelectron.* **2018**, *99*, 493−499.
(38) Chen, J.; Zheng, J.; Zhao, K.; Deng, A.; Li, J. *Chem. Eng. J.* **2020**, *392*, 123670.
(39) Wang, Y.; Zhao, G.; Chi, H.; Yang, S.; Niu, Q.; Wu, D.; Cao, W.; Li, T.; Ma, H.; Wei, Q. *J. Am. Chem. Soc.* **2021**, *143* (1), 504−512.

https://doi.org/10.1021/acs.analchem.2c03238
Anal. Chem. 2022, 94, 12280−12285